Particle Drift Induced by a Bubble in a Liquid-Solid Fluidized Bed with Low-Density Particles

K. Tsuchiya, G.-H. Song, W.-T. Tang, and L.-S. Fan
Dept. of Chemical Engineering, The Ohio State University, Columbus, OH 43210

In gas-liquid-solid fluidized beds used as bioreactors, the solid phase usually consists of either polymeric gel particles with enzymes or living cells entrapped in the internal porous structure or particles with biofilms attached to the surface. With the density of the particles (usually 1,020–1,300 kg/m^3) very close to that of the liquid, these bioparticles exhibit hydrodynamic characteristics different from high-density particles such as nonhomogeneity of axial-phase holdups distribution and small axial liquid dispersion (Tang and Fan, 1987, 1990). Tang and Fan (1987) developed a mechanistic model for predicting the axial solids distribution based on the vertical transport of the particles via the "bubble-engagement" region. This region, distinct from the particulate fluidization region, contributes to the overall effects due to the bubble wake and drift.

While a comprehensive summary describing the fluid dynamic behavior of the bubble wake is recently available (Fan and Tsuchiya, 1990), only scattered information on the drift effect can be found in the literature. The term "drift" was used first by Darwin (1953) to designate the deformation of material surfaces occurring in the irrotational flow of fluid past a solid body or, equivalently, induced by the translation of a body through an otherwise stationary ideal fluid. After the passage of the body, there is net movement of fluid elements in the direction of the body motion; the drift quantifies the ultimate displacement of each element in that direction. The drift volume, defined as the volume enclosed between the initial and final positions of the material surface, equals the hydrodynamic or added mass divided by the fluid density (Darwin, 1953).

Miyahara et al. (1989) observed that for a large bubble in a water 774-μm-glass-bead ($\rho_s = 2{,}500$ kg/m^3) fluidized bed, the particles moved upward above the upper free surface of the bed due to both the near-/primary-wake capture and the drift effect. The particle entrainment caused by the drift effect, however, was confined to the vicinity of the bed surface and was regarded insignificant. Even for successive bubbles, they confirmed the dominance of the primary-wake effect over the drift effect on the maximum vertical displacement of entrained particles. The principal role of the primary wake was also incorporated in the model for solids entrainment and deentrainment by El-Temtamy and Epstein (1980).

In the study on the wakes of drops in a stream, Yeheskel and Kehat (1971) noted that in addition to the wake-captured liquid, a significant amount of the surrounding liquid flowed upward (due to the drift effect). The total volume of liquid translated through the successive drops over a short distance was as high as 32 times the volume of the drops, more than an order of magnitude greater than the volume of liquid carried in the primary wake of single drops. Yeheskel and Kehat, however, found that the velocity of translation via drift was only about one-third of that of the drops (and thus of the wake). Anderson and Pratt (1978) made a similar observation for multiple drops dispersed in a liquid. These observations imply that for bubbles introduced successively into a liquid, the contribution of the drift effect is more significant than that of the wake effect with regard to the amount of the continuous-phase being transported. For bubbles in a liquid-solid medium, the amount of the solids being transported would also depend on the density of the particles due to gravitational settling.

Weber and Bhaga (1982) studied the drift effect induced by a large isolated bubble rising with its closed laminar wake in viscous liquids ($\mu_l = 82 - 2{,}800$ mPa·s). They indicated that the drift can be estimated based on the trajectories of liquid elements around an imaginary body encompassing the bubble and its attached/primary wake. Treating this enclosed region as a single body, referred to as a bubble-wake (Tsuchiya and Fan, 1988), is conceptually sound even for unstable open wakes and is often useful in describing various flow/transport phenomena in multiphase systems (Fan and Tsuchiya, 1990). Weber and Bhaga found that in contrast to the drift caused by a wakeless body (Darwin, 1953; Lighthill, 1956), the drift by a rising bubble—when viewed in terms of the trajectories of

Correspondence concerning this article should be addressed to L.-S. Fan.
Current address of: K. Tsuchiya, Department of Chemical Science and Technology, The University of Tokushima, Tokushima 770, Japan; G.-H. Song, Polyolefins Division, Union Carbide Corporation, Technical Center, P.O. Box 8361, South Charleston, WV 25303; and W.-T. Tang, Shell Development Company, Westhollow Research Center, Houston, TX 77082.

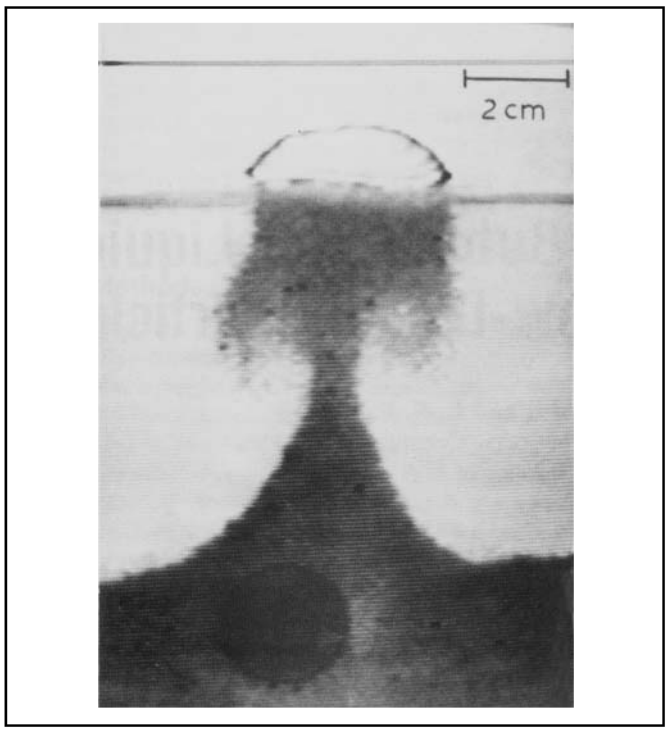

Figure 1. Circular-cap bubble, whose primary wake visualized through entrapped particles and associated particle drift in a water-calcium alginate particle fluidized bed.

individual elements—was not symmetric about the traversing plane of the maximum lateral displacement of the elements from the axis of bubble rise. The extent of drift was larger after the bubble overtook the elements. This "enhancement" of drift is probably due to the effect of the secondary wake behind the bubble-wake. Note that the pressure behind the bubble-wake cannot completely recover even in the secondary wake of thin thread (Fan and Tsuchiya, 1990). The secondary-wake effect was also seen in that the final lateral positions of

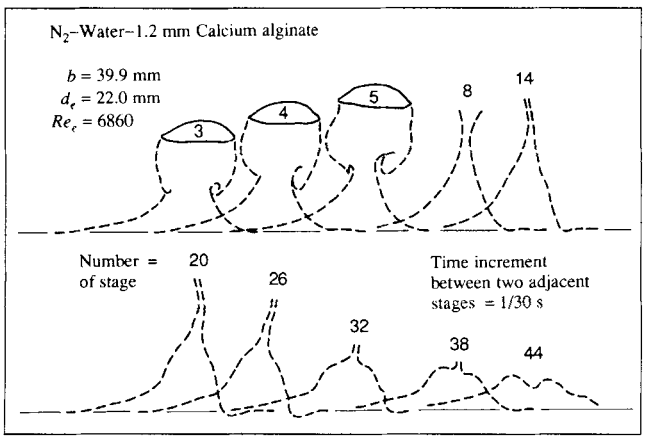

Figure 2. Sequence of particle entrainment and de-entrainment by a single bubble into the freeboard of a water-calcium alginate particle fluidized bed.

the drifted elements became closer to the axis of rise than their initial positions as the bubble Reynolds number, Re_e, increased (Weber and Bhaga, 1982).

The objective of this note is to examine the effect of solid density on the particle drift in gas-liquid-solid fluidization. Two types of particles are used: 774-μm glass beads as high-density particles and 1.2-mm calcium alginate particles which simulate low-density bioparticles. The effective drift is evaluated by measuring the apparent amount of drifted particles above the free surface of the liquid-solid fluidized bed.

Experimental Studies

A rising bubble, its near wake and the resulting drift of particles above the upper free surface of a liquid-solid fluidized bed are observed through a video camera which can move vertically at speeds varying from 0 to 0.6 m/s. A two-dimensional Plexiglas column is used in the experiments; the column is of 1.4-m height, 0.305-m width and 8-mm nominal gap thickness. Details of the liquid distributor, the bubble injection system and the camera transport system are given elsewhere (Tsuchiya and Fan, 1986; Tsuchiya et al., 1990).

Nitrogen and tap water are used as the gas and liquid phases, respectively. Two types of particles are used as the fluidized solid phase: (1) calcium alginate particles of averaged diameter 1.2 mm and density 1,020 kg/m^3; (2) glass beads of diameter 774 μm and density 2,500 kg/m^3. The detailed procedure for preparing the calcium alginate particles is reported elsewhere (Tzeng et al., 1991).

Results and Discussion

Experimental observations

Miyahara et al. (1989) presented a series of photographs which reflect the dynamics of particle entrainment and de-entrainment by a single bubble into the freeboard of a two-dimensional liquid-solid fluidized bed. In their photographs, the extent (effective height) of particle carryover through the drift appeared less significant than that via the bubble wake. The photograph shown in Figure 1, on the other hand, reflects the significant role of the drift in particle carryover. The liquid velocity employed is 0.4 mm/s. The main difference between Miyahara et al.'s and the present cases lies in the particle properties, specifically in the particle density. It is thus essential to include the contribution of the drift effect on the particle carryover in a fluidized bed with low-density particles.

While Figure 1 gives a still picture for a circular-cap bubble, its primary wake (viewed through the entrapped particles) and the associated particle drift, the time evolution of them, particularly of the drift, are sketched in Figure 2 for the same bubble and alginate particles. In the figure, the flow in each stage is viewed in the frame of reference fixed at a particular flow region: at the bubble when it drives the particle flow; at the drifted particles otherwise. The sequence of stages, however, is constructed in the reference frame fixed at the upper free surface of the liquid-solid fluidized bed, the bubble thus ascending at the rate $U_b + U_l$, that is, its terminal rise velocity plus the superficial liquid velocity. The time increment between two adjacent stages is 1/30 s with stage 0 corresponding to the moment of bubble emergence into the freeboard. For a given large bubble [with the breadth (b) as large as 40 mm], the primary wake exhibits quasi-stable symmetric structure (see

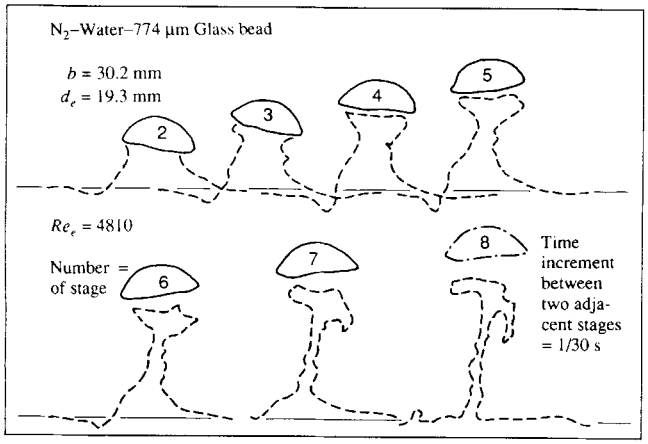

Figure 3. Sequence of particle entrainment and de-entrainment by a single bubble into the freeboard of a water-glass bead fluidized bed.

the first three stages in Figure 2), despite its inherent vortex-shedding characteristics (Fan and Tsuchiya, 1990). The boundary of the bubble wake is roughly a circle or a slightly elongated (prolate) oval shape. It, therefore, seems appropriate to treat the region of dragged particles "diverging" downstream as particles drifted due to the rise of the round-shape bubble wake. The particle drift proceeds with the bubble rise and ideally, that is, when the particle inertia is sufficiently small so that the particles are indistinguishable from the liquid elements, the final profile of the drift should be stationary with respect to the uniform liquid flow. For the alginate particles of low density as in Figure 2, the drift indeed exhibits a profile appearing for some time, but gradually collapsing due to non-negligible gravity settling. The highest collapsing rate occurs next to the wake central axis (see stages 32–44 in Figure 2).

Figure 3 shows similar sketches for heavier glass beads. In this case, the particle drift never reaches a quasi-stable profile; the collapsing stage begins while the profile is being established (see stages 5 and 6) due to higher settling velocity. Along the wake central axis, however, some particles remain suspended in the form of a thin stream—though their contribution to the total amount of drift is insignificant—even after the main part of the drift has been settled back to the bed (see stages 7 and 8). Actually, this portion contains the particles that are originally carried by the primary wake and are then gradually draining along the streaming path preferentially. Evidently, the amount of solids transported via the primary wake, estimated from the apparent projected area of high solids concentrations in that region, is smaller and progressively decreasing. This area corresponds to the confined turbulent wake region (Fan and Tsuchiya, 1990), specifically the stable solids wake region (Kitano and Fan, 1988).

Figure 4 compares the extents of particle drift between the light- and heavy-particle cases; the time variation in the drift area—the area enclosed between the initial position of the material surface (assumed to coincide with the flat line connecting the left and right edges of the upper free surface of the bed at the given time) and the position at the given time—normalized with the bubble area (k_D) is plotted against the elapsed time. The distinctive difference in the drift behavior between the light and heavy particles lies not only in the amount of the particles being drifted but, more profoundly, in the length of period in which the drift pattern can be maintained. This latter aspect is demonstrated in Figure 4 by comparing the data for the large bubbles ($d_e \approx 20$ mm). While the maximum attainable drift areas in both cases are comparable ($k_D = 4.3$ and 2.7 for the calcium alginate particles and the glass beads, respectively), the length of period differs drastically: for the maintenance of the drift area above 80% of the maximum value, the former spans up to 0.8 s, the latter merely less than 0.1 s. This difference yields some hydrodynamic characteristics observed in gas-liquid-solid fluidized-bed bioreactors; for example, the longer the particle drift persists, the greater the likelihood for these particles being captured by the successive bubbles at higher locations, leading to more axial solids transport.

The maximum attainable k_D evaluated in this study is plotted vs. the bubble size d_e in Figure 5 along with the normalized primary wake/stable solids wake area (whichever applies from the viewpoint of solids carryover). The difference in k_D between the two types of particles is particularly large for small bubbles. The difference, however, appears to diminish as the bubble size increases. The distinctively large amount of the light par-

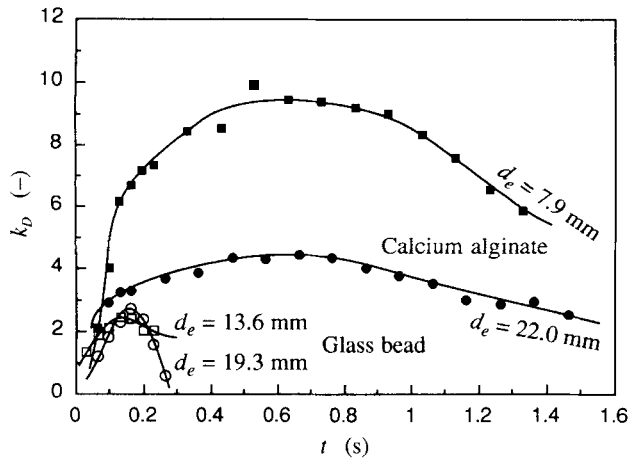

Figure 4. Time variation in normalized particle drift area in the freeboard of a water-solid fluidized bed.

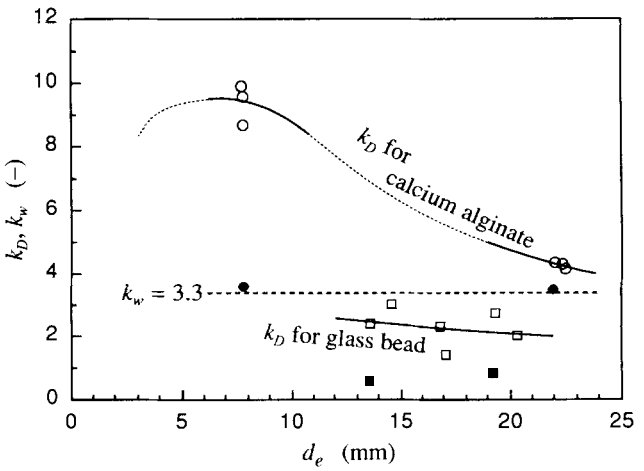

Figure 5. Maximum attainable particle drift area (○, □) and effective wake area (●, ■) as functions of bubble diameter.

ticles entrained as "apparent" drift behind small bubble-wakes is speculated to be due to a high degree of openness of the wake. Although not confirmed in this study, the particles are expected to ascend faster after they have been passed by the rising bubble (Weber and Bhaga, 1982). This enhancement effect, which is absent for wakeless bodies, is especially strong when the secondary wake works as an efficient pressure sink. For bubbles with appreciable oscillations and thus with vigorously fluctuating primary wakes, their secondary wakes can be full of still strong vortical structures shed from the primary wake, providing sufficient pressure driving force for an extra pull of particles. The bubbles of d_e ranging from 5 to 10 mm are observed to provide this enhancement effect. If the particles are heavy, this extra contribution may not be so effective.

The effective wake area (k_w, normalized) is estimated in relatively short elapsed times ($t \sim 0.1$ s). For the low-density particles, k_w values obtained for two specific bubble sizes are approximately the same (≈ 3.5), which indeed fall in the range of the primary-wake area for in-bed bubbles obtained by Tsuchiya and Fan (1986), that is, $k_{pw} = 3.3 \pm 1.2$ (see the dashed line in Figure 5), as suggested by Miyahara et al. (1989). This coincidence, however, may not apply to the k_w for the high-density particles estimated in this study. Within a short time interval on an order of 1/10 s, the particles in the primary wake have appreciably fallen downstream (see Figure 3), leading to noticeably small values of $k_w (< 1)$.

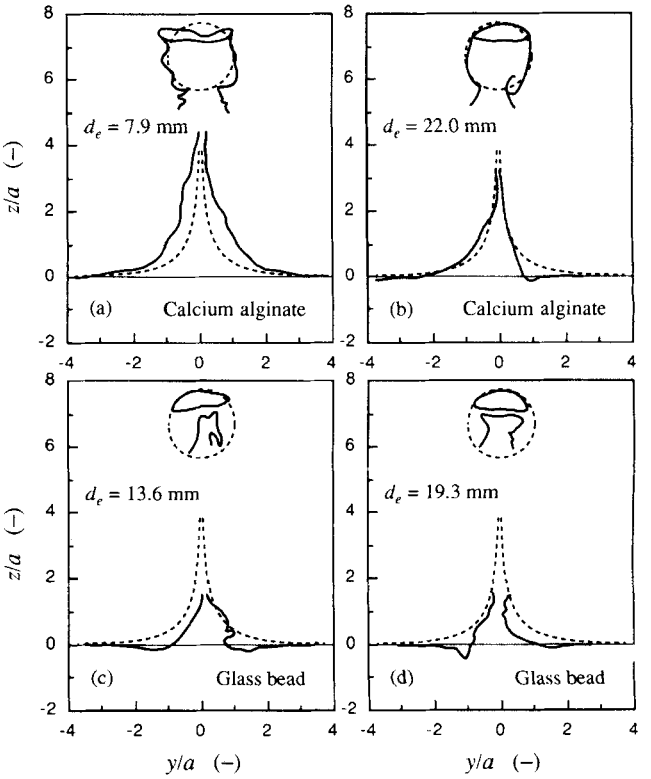

Figure 6. Comparison of experimental drift profiles (—) with theoretical profile (- - - -) based on the potential flow model of Darwin (1953).

Potential flow model

Darwin (1953) derived a theoretical relationship for the drift induced by a solid body moving uniformly through an ideal fluid: for a circular cylinder, that is, for a two-dimensional case, the drift area normalized with the circle area is found to be unity. This finding is translated to:

$$k_D = 1 + k_{pw} \tag{1}$$

for the present system with the bubble-wake assumed to be circular. Here, the primary-wake size k_{pw} is used instead of the net particle-containing wake size k_w, since the primary wake defines more closely the part of the true hydrodynamic boundary of the combined bubble-wake (Tsuchiya and Fan, 1986).

If the constant value of $k_{pw} = 3.3$ of Tsuchiya and Fan (1986) is adopted, the ideal drift area—the drift of the surrounding medium (thus with no "excess" inertia) caused by a wakeless body (thus with no secondary-wake effect)—would have a value $k_D = 4.3$. This value, when compared to the present experimental results, can give a reasonable estimate for the low-density calcium alginate particles drifted by large bubbles ($d_e = 22$ mm) with rather stable primary wakes. Note that the k_D values in Figure 5 for three such bubbles are 4.32, 4.28, and 4.14. For the same particles, but when associated with the smaller bubbles ($d_e = 8$ mm), the experimental values are as high as twice the value predicted by the potential flow model. Since the particle settling is expected to occur to the same extent as that for the large bubble case, this increase in the drift area should come from the extra pull associated with the remnant pressure defect behind the primary wake. For the high-density glass beads, experimental k_D ranging from 1.4 to 3.0 is less than the theoretical value, indicating appreciable particle settling due to high inertia as evidenced in Figure 3 or 4.

Further comparisons of the experimental data with the potential flow model can be made in terms of the actual drift profile. Figure 6 shows such comparisons for four representative cases: (a) small and (b) large bubbles with the light calcium alginate particles; (c) small and (d) large bubbles with the heavy glass beads. In all the cases, the sketches of the bubble and its primary wake (particle-containing part) are made at the elapsed time $t = 0.133$ s, four stages after the bubble emergence. The sketches of the drift profile, represented by the uppermost particles (but below the primary-wake particles) entrained into the freeboard, are made at the times which give the maximum attainable drift area: (a) 0.533 s, (b) 0.467 s, (c) 0.133 s, and (d) 0.167 s. Also note that the dimensions are so normalized that the average area of the bubble-wake—evaluated at the earlier elapsed times using Eq. 1 with $k_{pw} = 3.3$ and with the average bubble area evaluated at several locations in both the in-bed and freeboard regions—coincides with the theoretical area of a circle whose radius is unity.

As shown in Figures 6a and 6b, the shape of the experimentally observed drift profiles for the light particles resembles that of the theoretical profile, despite some irregularity and asymmetry. The theoretical curve in Figure 6 corresponds to the analytical solution presented by Darwin (1953) for the stream function for a potential flow around a circular cylinder:

$$\psi = (U_b + U_l) y \left(1 - \frac{a^2}{y^2 + z^2}\right) \tag{2}$$

in the reference frame fixed at the cylinder. In particular, the drift in Figure 6b induced by the large bubble has a pattern (if disregarding the slight asymmetry) and an area almost identical to the theoretical ones. The sketched boundary of the bubble-wake in this case also closely follows the theoretical circular pattern. The corresponding boundary for the small bubble case (Figure 6a), however, largely deviates from the circle. Note that the bubble shape was observed to drastically change with time, as indicated in Figure 6a, justifying the proposed mechanism of the secondary-wake effect on the drift enhancement described earlier. For the heavy particles (Figures 6c and 6d), on the other hand, the pattern of the drift profile is deformed with appreciable deviations from the theoretical one.

Concluding Remarks

The visual study on the effect of solid density on the particle drift induced by a rising bubble in the freeboard of a liquid-solid fluidized bed shows that significant differences exist in the drift behavior between fluidized particles of a high density (for example, 2,500 kg/m^3 glass beads) and of a low density (for example, 1,020 kg/m^3 calcium alginate). While the glass beads never attain the (steady-state) drift profile, characteristic of fluid elements in a homogeneous medium, the low-density calcium alginate particles exhibit quasi-stable profiles over a prolonged period. Consequently, the amount of drift or the drift area, especially in an integrated (with respect to time) sense, is much greater for the low-density particles than for the high-density particles.

The maximum attainable drift area for both particles is compared with the theoretical drift area predicted based on a simple potential flow model. It is found that for the light particles, the drift area normalized with respect to the area of the bubble-wake, which includes the bubble and the hydrodynamically defined primary wake, coincides with the theoretical value, when the bubble-wake is stable as in large bubbles. When the bubble-wake is unstable as in small bubbles for the same particles, the normalized drift area tends to increase due to the extensive secondary-wake effect associated with the wake open structure; the remnant pressure defect behind the bubble-wake can provide an extra pull of the downstream particles. The present results imply that for gas-liquid-solid fluidized-bed bioreactors containing low-density particles, the upward solids transport can be contributed not only by the particles trapped in (and shed from) the primary wake but also very significantly, by the drift resulting from the successive bubbling.

Acknowledgment

This work was sponsored by the NSF Grant CTS-9200793.

Notation

a = radius of a translating circular cylinder
b = bubble breadth
d_e = equivalent bubble diameter: diameter of a circle having the same area as the bubble
k_D = ratio of drift area to bubble area
k_{pw} = ratio of primary-wake area to bubble area
k_w = ratio of effective (particle-containing) wake area to bubble area
Re_e = bubble Reynolds number based on the equivalent bubble diameter $= d_e U_b \rho_l / \mu_l$
t = time elapsed from the moment of bubble emergence into the freeboard
U_b = bubble terminal velocity: bubble rise velocity relative to the liquid phase
U_l = superficial liquid velocity
y = horizontal righthand distance from the axis of bubble rise
z = vertical upward distance from the upper free surface of the fluidized bed

Greek letters

μ_l = liquid viscosity
ρ_l = liquid density
ρ_s = solid density
ψ = stream function for particle flow

Literature Cited

Anderson, W. J., and H. R. C. Pratt, "Wake Shedding and Circulatory Flow in Bubble and Droplet-Type Contactors," *Chem. Eng. Sci.*, **33**, 995 (1978).

Darwin, C., "Note on Hydrodynamics," *Proc. Camb. Phil. Soc.*, **49**, 342 (1953).

El-Temtamy, S. A., and N. Epstein, "Simultaneous Solids Entrainment and De-entrainment Above a Three-Phase Fluidized Bed," *Fluidization*, J. R. Grace and J. M. Matsen, eds., p. 519, Plenum Press, New York (1980).

Fan, L.-S., and K. Tsuchiya, *Bubble Wake Dynamics in Liquids and Liquid-Solid Suspensions*, Butterworth-Heinemann, Stoneham (1990).

Kitano, K., and L.-S. Fan, "Near-Wake Structure of a Single Gas Bubble in a Two-Dimensional Liquid-Solid Fluidized Bed: Solids Holdup," *Chem. Eng. Sci.*, **43**, 1355 (1988).

Lighthill, M. J., "Drift," *J. Fluid Mech.*, **1**, 31 (1956).

Miyahara, T., K. Tsuchiya, and L.-S. Fan, "Mechanism of Particle Entrainment in a Gas-Liquid-Solid Fluidized Bed," *AIChE J.*, **35**, 1195 (1989).

Tang, W.-T., and L.-S. Fan, "Hydrodynamics of a Three-Phase Fluidized Bed Containing Low Density Particles," *AIChE J.*, **35**, 355 (1989); Paper 150d, AIChE Meeting, New York (Nov. 15–20, 1987).

Tang, W.-T., and L.-S. Fan, "Axial Liquid Mixing in Liquid-Solid and Gas-Liquid-Solid Fluidized Beds Containing Low Density Particles," *Chem. Eng. Sci.*, **45**, 543 (1990).

Tsuchiya, K., and L.-S. Fan, "Near-Wake Structure of a Single Gas Bubble in a Two-Dimensional Liquid-Solid Fluidized Bed: Vortex Shedding and Wake Size Variation," *Chem. Eng. Sci.*, **43**, 1167 (1988); Paper 10b, AIChE Meeting, Miami Beach (Nov. 2–7, 1986).

Tsuchiya, K., and L.-S. Fan, "Prediction of the Wake Size of a Single Gas Bubble in Liquid and/or Liquid-Solid Media—the Pendulum Model," *Chem. Eng. Sci.*, **43**, 2893 (1988).

Tsuchiya, K., G.-H. Song, and L.-S. Fan, "Effects of Particle Properties on Bubble Rise and Wake in a Two-Dimensional Liquid-Solid Fluidized Bed," *Chem. Eng. Sci.*, **45**, 1429 (1990).

Tzeng, J.-W., R.-H. Jean, and L.-S. Fan, "Bed Expansion Characteristics of Liquid Fluidization with Calcium Alginate Beads," *J. Chinese Inst. Chem. Eng.*, **22**, 329 (1991).

Weber, M. E., and D. Bhaga, "Fluid Drift Caused by a Rising Bubble," *Chem. Eng. Sci.*, **37**, 113 (1982).

Yeheskel, J., and E. Kehat, "Wakes of Vertical and Horizontal Assemblages of Drops," *Chem. Eng. Sci.*, **26**, 2037 (1971).

Manuscript received Apr. 6, 1992, and revision received July 24, 1992.